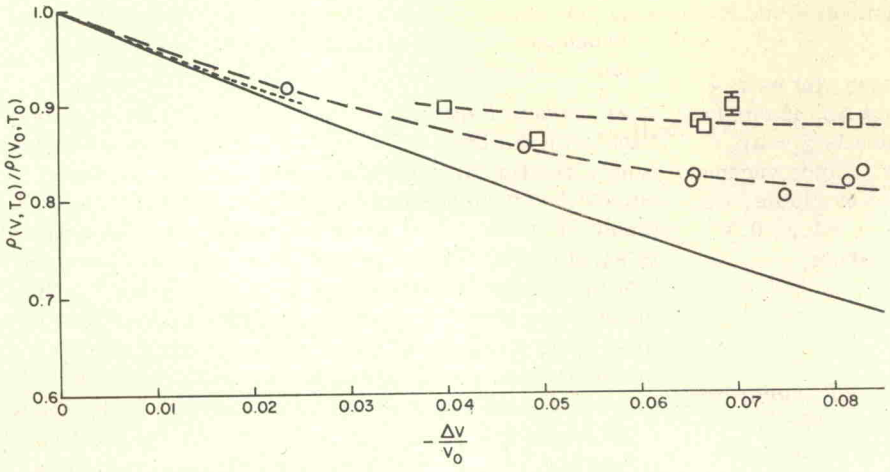

FIG. 8. Isothermal resistivity vs compression. Solid line, calculated hydrostatic resistivity fitted to initial pressure derivative of Goree and Scott (Ref. 17); dotted line, Bridgman's hydrostatic results; dashed lines, fits to experimental data of different purity; □, purer W3N silver; ○, MRC silver.

ture by an amount depending on shock strength, it is necessary to convert the shock resistance change data to isothermal resistivity before comparing them to hydrostatic experiments and theory. Conversion was done using calculations of temperature and temperature coefficient of resistance described in Sec. III.

Since the voltage-time profiles were not square pulses, some judgment was necessary in picking representative values for use in plotting data. The best-characterized point on the profile seemed to be at the end of the viewing window, $\frac{1}{2}$ μsec after shock arrival at the foil. Since on many records a more or less steady level had been reached by this time, this value was used for computing ρ/ρ_0 data points.

Isothermal resistivity of silver as a function of compression is shown in Fig. 8. All shock data lie well above the calculated hydrostat. Estimated uncertainties in temperature, temperature coefficients of resistivity, and hydrostatic resistivity extrapolation do not account for the difference. Shock results for different purity silver also differ and there may be a small effect of annealing prior to shocking for the less pure silver (Fig. 9).

Deviation of the shock isothermal resistivity from hydrostatic results is attributed mainly to resistivity of lattice defects (mainly vacancies) generated by plastic deformation associated with passage of the shock wave. This defect resistivity is given by

$$\frac{\Delta\rho_D}{\rho_0} = \frac{[\rho(V,T_0)]_{\text{Expt}} - [\rho(V,T_0)]_{\text{Calc}}}{\rho(V_0,T_0)},$$

where $[\rho(V,T_0)]_{\text{Calc}}$ comes from Eq. (5). (Also see Figs. 8 and 9.) Metals which have been shocked and relieved back to ambient conditions also show evidence of this increased lattice imperfection by changes in microstructure and hardness, and in results of annealing studies.[4–6,29–33]

If we accept the above interpretation of the deviation, the number of defects generated by the shock is quite large. Figure 9 shows the excess resistivity $\Delta\rho_D/\rho_0$ of the shock data as a function of pressure. At 100 kbar $\Delta\rho_D/\rho_0 = 0.099$ for MRC silver and 0.158 for W3N silver. In comparison, shock conductivity data of Keeler and Royce[34] for copper and iron result in $\Delta\rho_D/\rho_0 = 0.12$ and 0.16, respectively. (They corrected their data for shock temperature rise but details of the calculation were not published.)[35]

E. Defect concentrations and production

Imperfections produced by shock deformation will likely include combinations of vacancies, interstitials, dislocations, and possibly deformation twins. Experiments indicate that vacancies are formed in preference to interstitials in face-centered-cubic (fcc) metals,[4,6,31,32,36] and electron microscopy of shocked and recovered aluminum and nickel gives some evidence for prismatic dislocation loops formed by the collapse of vacancy clusters.[6,32] Of the various defects, the production of vacancies appears to be the most economical way of increasing the resistivity in fcc metals. Interstitials or dislocations require roughly three to seven times as much energy of formation as vacancies for the same resistivity change; estimates of formation energy and specific resistivity were taken from Cotterill and Doyama,[37] and Martin and Paetsch,[38] respectively, for

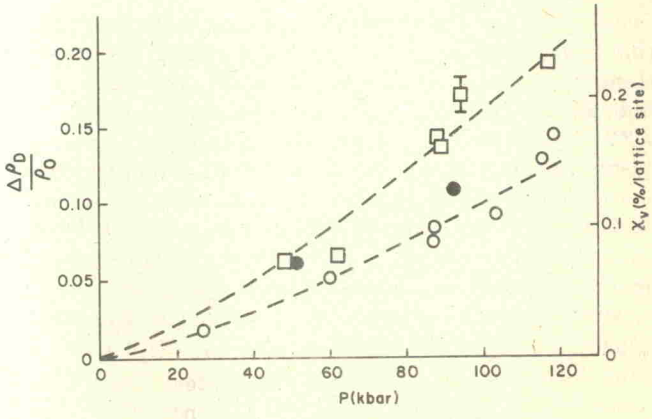

FIG. 9. Excess resistivity and vacancy concentration vs pressure. Dashed line, fit to experimental data of different purity; □, purer W3N silver; ○, annealed MRC silver; ●, unannealed MRC silver.

interstitials and from Cottrell[39] and Basinski *et al.*,[21] respectively, for dislocations.

To find approximate defect concentrations, let us assume for simplicity that excess resistivity $\Delta\rho_D$ is due to vacancies. The vacancy concentration then is $\chi_v = \Delta\rho_D/\rho_v$ where ρ_v is the resistivity per vacancy. Since vacancy resistivity as a function of pressure is not available, we will use the vacancy resistivity at 1 atm, $\rho_v = 1.3 \pm 0.7$ $\mu\Omega$ cm/at.% for silver.[40] Since $\rho_0 = 1.6$ $\mu\Omega$ cm

$$\chi_v = \frac{\Delta\rho_D}{\rho_0}\frac{\rho_0}{\rho_v} \approx 1.2\times10^{-2}\frac{\Delta\rho_D}{\rho_0}.$$

Using the 100-kbar shock data for MRC silver, computed vacancy concentration is then about 10^{-3} vacancies/atomic site (Fig. 9). Concentrations are higher in the purer W3N silver. Defect concentrations generated by severe torsion deformation or radiation damage by electrons below 20 °K are also of this magnitude.[41,42] Estimates of equilibrium vacancy concentration at the melting points of metals range as high as 10^{-2}.[43] For temperatures and pressures in shocked states of the present work, concentrations of the order of 10^{-3} correspond to strongly nonequilibrium defect concentrations. The shock experiments correspond to damage experiments at cryogenic temperatures in that defects generated do not migrate to the surface in either case. In the cryogenic case the constraint is low thermal energy of the solid; in the shock case it is the short time scale of the experiments.

For a given strain these concentrations are about two orders of magnitude higher than those found in low strain rate deformation.[44] This fact may indicate the existence of dislocation speeds near shear-wave speed since relativistic dislocations are expected to be much more efficient producers of points defects,[45] the mechanism being nonconservative motion of jogs on dislocations.[36,46]

A plot of $\ln(\Delta\rho_D/\rho_0)$ vs $\ln(-\epsilon)$ shows point-defect concentration is approximately proportional to the three-halves power of total strain ϵ; compressive strains and stresses are negative. For the expression $\chi_v = A(-\epsilon)^n$ the results for W3N silver are $A = 0.14$, $n = 1.58$ and for MRC silver are $A = 0.051$, $n = 1.46$.

F. Energy balance

One important check on the assertion that deviation from hydrostatic resistivity is due to defect resistivity is energy balance. Was enough plastic work done to generate the defect concentrations calculated in Sec. IV E? At 100 kbar an elementary calculation of work of plastic deformation[47] gives 3.9 bar cm^3/g; this was based on a Hugoniot elastic limit of 1.2 kbar calculated from a yield stress in tension of 0.5 kbar and on a work-hardening modulus of 14 kbar.[48] At 1 atm of pressure, vacancy formation energy in silver is 1.8×10^{-12} erg/vacancy.[49] As with vacancy resistivity, the dependence of monovacancy formation energy on pressure is not known. Using the 1 atm value for formation energy implies a total energy of formation of 11 bar cm^3/g for a monovacancy concentration of 10^{-3}, 2.8 times larger than the work of deformation calculated. An additional difficulty is that a majority of the work of deformation is believed to be dissipated as heat. Given these facts, an average Hugoniot elastic limit of 10–20 kbar in the first 20 μm of shock propagation in silver would be necessary to balance energy for a 100-kbar shock.

An aspect of shock response of solids which is relevant to the problem of energy balance is stress relaxation in elastic-plastic solids. For a stress relaxing solid it has been postulated that initial elastic stress in the solid at the face where the shock enters the material is equal to the total stress acting on the face, provided that the loading wave has a very fast rise time.[50] This means very high initial stresses on the dislocations in their glide planes. As the shock propagates into the material, the elastic stress relaxes with time and distance to a steady-state level characteristic of the shock response of that solid. At the same time the plastic strain is gradually accommodated by dislocation glide, multiplication, nucleation, and by twinning. If such behavior occurs in the first 20 μm of shock-wave propagation in the silver used, it is not difficult to imagine an average elastic stress over distance and time which is a sizeable fraction of a 100-kbar driving stress.

G. Effect of purity on shock-induced vacancy concentrations

Figure 9 shows the effect of purity on resistivity deviation and vacancy concentrations generated. Higher vacancy concentrations are generated in the purer silver (W3N). This effect of purity is opposite to low strain rate deformation results where, when a purity effect is noted, there is more resistivity change for lower-purity material.[51–53] Resistance ratios between room temperature and 4.2 °K indicate that W3N silver specimens have an impurity concentration about half that existing in MRC specimens. (MRC silver was specified as 5N and W3N silver as 3N pure by the supplier.)

Effect of purity has been noted in other shock experiments. Experiments in lithium fluoride by Asay *et al.*[50] showed quasistatic yield stress to increase smoothly with initial defect concentration (either impurity atoms or irradiation-induced point defects). Shock experiments by the same workers and by Gupta *et al.*[54] on the same materials showed elastic precursor decay rate and plastic strain rate to depend on concentration of divalent impurities and on heat treatment.

A model based on stress relaxation for the effect of metal purity on shock-induced defect concentrations is currently being developed by the authors.[47]

H. Effect of anneal on shock resistivity

Part of the experimental program was to determine the effect of high-temperature annealing on the resistivity change of cold-rolled silver foil in response to shock waves. Two shots were done on unannealed MRC foil. Defect concentration data for the unannealed foil are slightly higher than for annealed (Fig. 9). More data would be necessary to know if this deviation is real.

Since most point defects in silver will annihilate or diffuse to the surfaces at room temperature,[55] the main effect of high-temperature anneal is removal of disloca-